Electronic Supplementary Material (ESI) for Catalysis Science & Technology.
This journal is © The Royal Society of Chemistry 2021

Supporting Information for

Rational Design of Interface Refining through Ti^{4+}/Zr^{4+} diffusion/doping and TiO_2/ZrO_2 Surface Crowning of $ZnFe_2O_4$ Nanocorals for Photoelectrochemical Water Splitting

Sarang Kim[a,‡], Mahadeo A. Mahadik[a,‡], Anushkkaran Periyasamy[a], Weon-Sik Chae[b], Jungho Ryu[c], Sun Hee Choi[d],* and Jum Suk Jang,[a,*]

[a]Division of Biotechnology, Advanced Institute of Environmental and Bioscience, College of Environmental and Bioresource Sciences, Chonbuk National University, Iksan 570-752, Republic of Korea.

[b]Daegu Center, Korea Basic Science Institute, Daegu 41566, Republic of Korea

[c]Geologic Environment Research Division, Korea Institute of Geoscience and Mineral Resources (KIGAM) Daejeon 305-350, Republic of Korea.

[d]Pohang Accelerator Laboratory (PAL), Pohang University of Science and Technology (POSTECH), Pohang 37673, Republic of Korea.

*Corresponding authors: Tel.: +82 63 850 0846; fax: +82 63 850 0834

E-mail address: shchoi@postech.ac.kr (S. H. Choi); jangjs75@jbnu.ac.kr (J.S. Jang)

‡Authors with equal contributions.

Figures

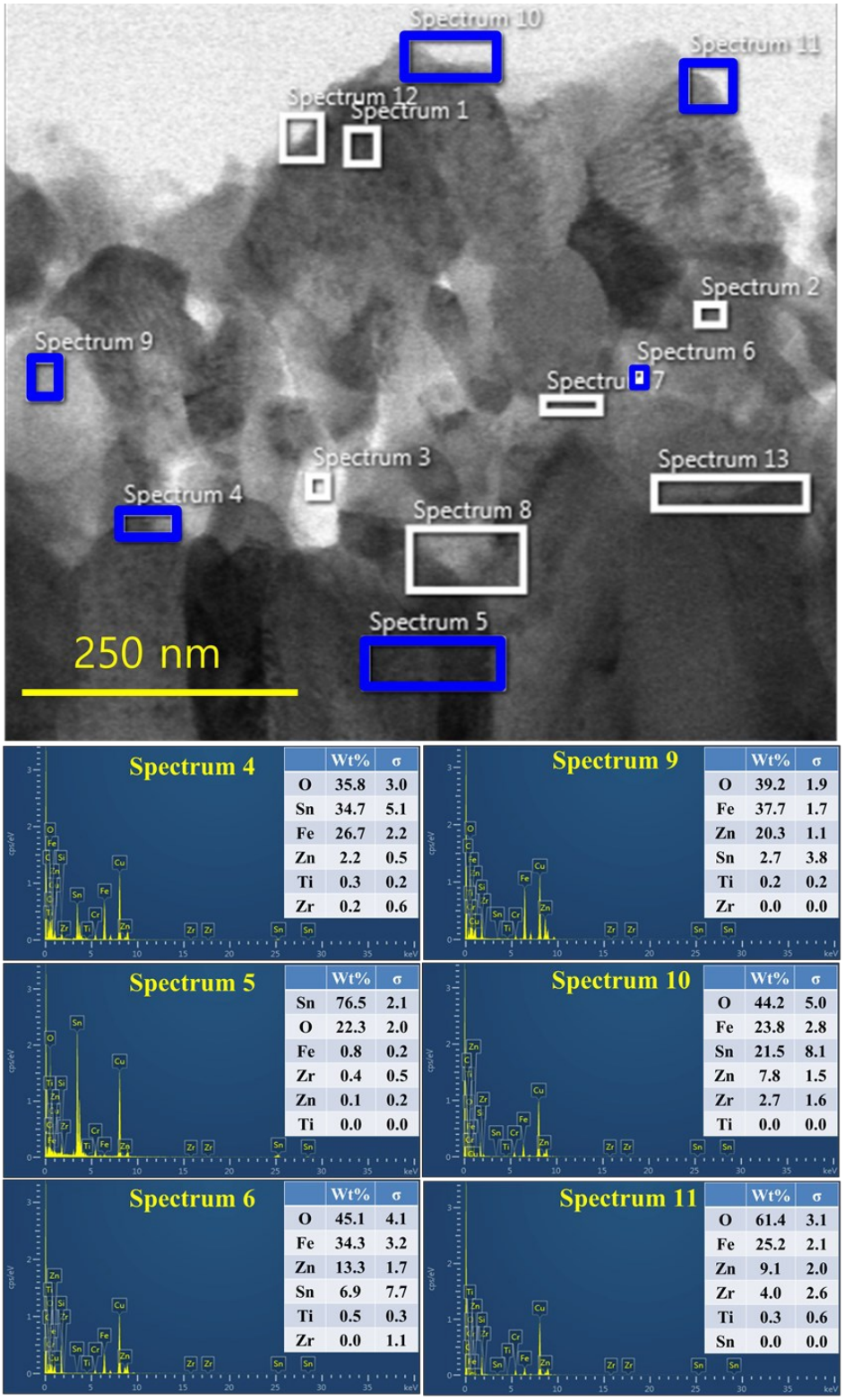

Fig. S1 TEM cross-sectional micrographs after FIB cutting of TZF-15 photoanodes with their respective EDS spectra, revealing the wt% compositions of Fe, O, Zn, Zr, Ti and Sn elements.

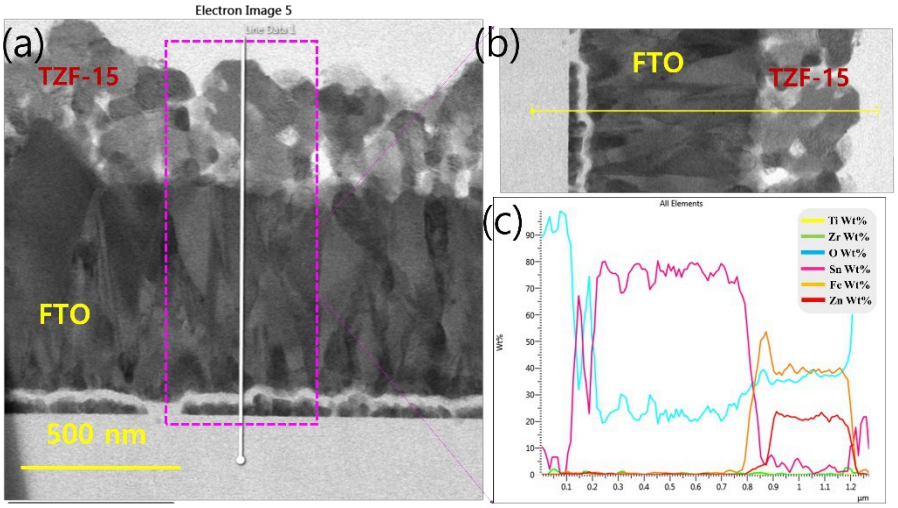

Fig. S2 (a) FIB-TEM cross-sectional micrographs of TZF-15 photoanode. (b, c) corresponding TEM-line profile gained from TEM-EDS analysis, revealing the diffusion/doping of Ti ions from TiO_2 underlayer.

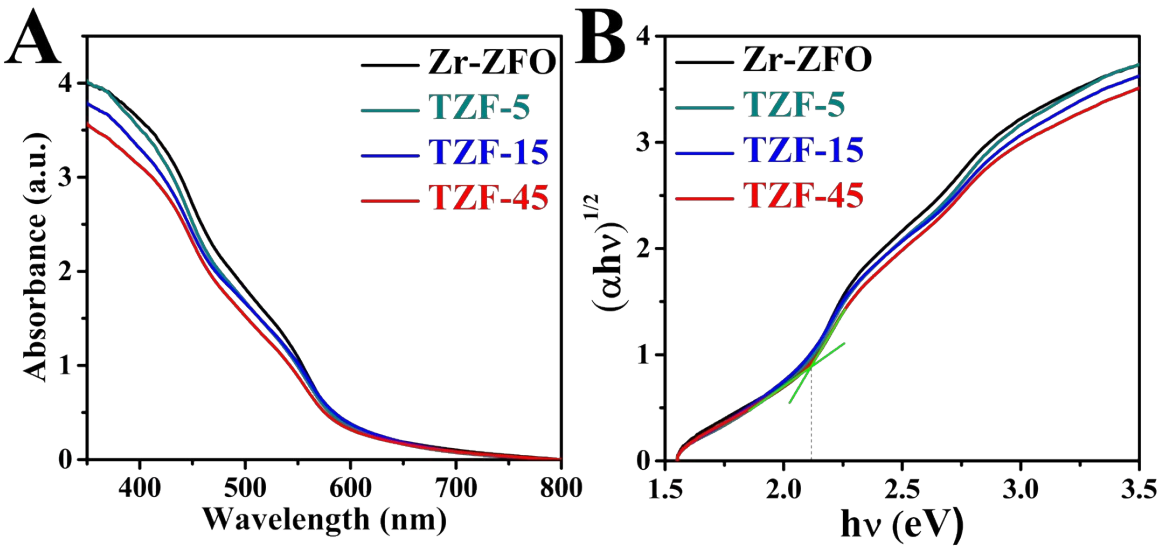

Fig. S3 (A) UV-vis absorbance spectra and (B) Tauc plots of Zr-ZFO, TZF-5, TZF-15 and TZF-45 photoanodes respectively.

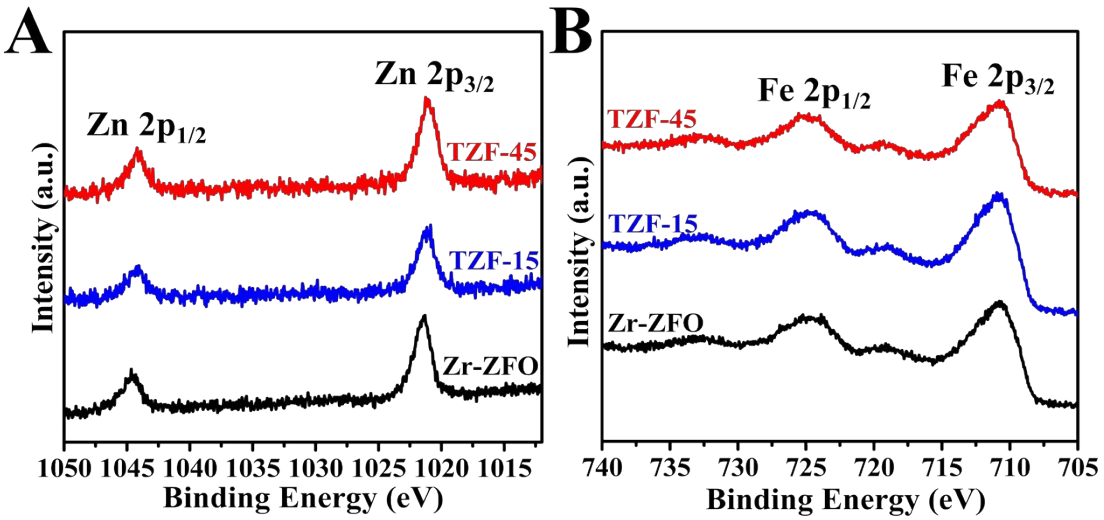

Fig. S4 XPS spectra of (A) Zn 2p and (B) Fe 2p for Zr-ZFO, TZF-15 and TZF-45 photoanodes respectively.

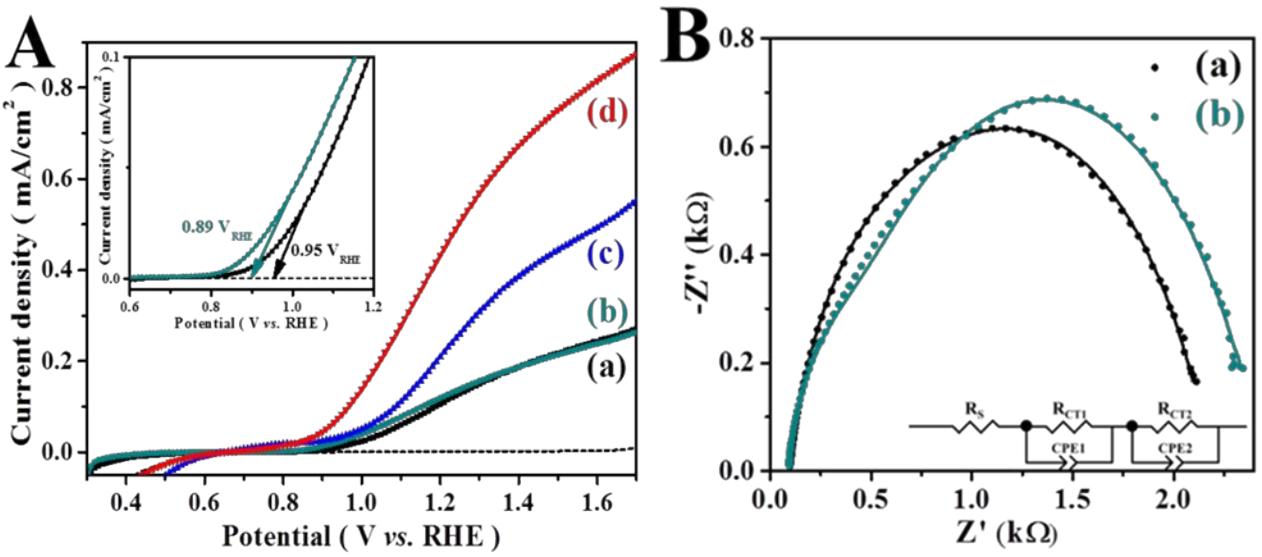

Fig. S5 (A) Photocurrent density–potential characteristics under light (solid lines)/in the dark (dashed lines) conditions for (a) pure ZFO, (b) pure ZFO with 15mM TiO_2 underlayer, (c) Zr-ZFO and (d) TZF-15 photoanodes. The onset potential of (a) pure ZFO, (b) pure ZFO with 15mM TiO_2 underlayer shown in the inset of Figure S5A. (B) Nyquist plots under light for (a) pure ZFO, (b) pure ZFO with 15mM TiO_2 underlayer photoanodes with the equivalent circuit for the EIS fitting (inset), the 1 M NaOH used as electrolyte solution.

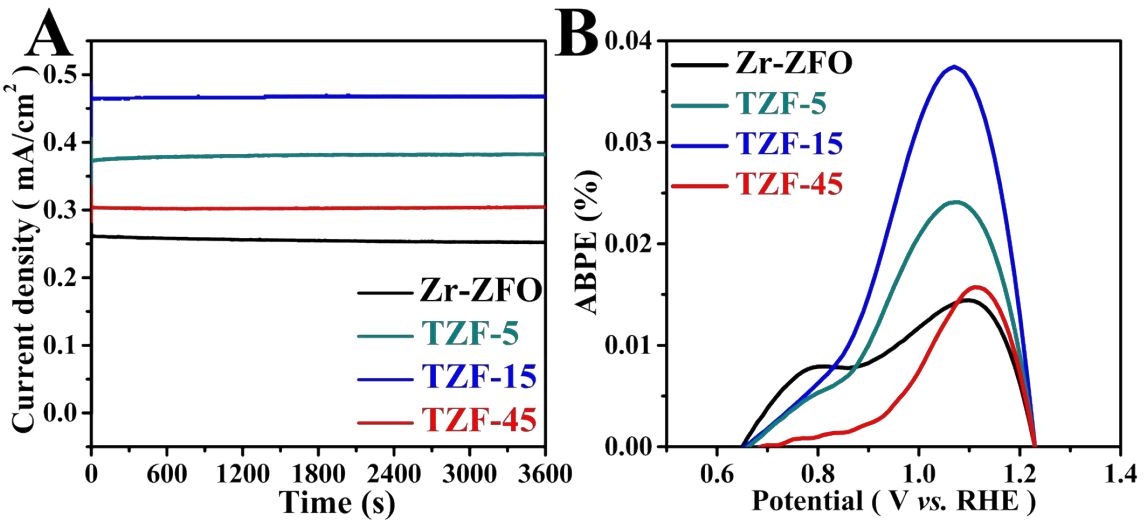

Fig. S6 (A) photo-stability test under 1 sun illumination condition using 1 M NaOH at 1.23 V *vs.* RHE and (B) Photoconversion efficiency as a function of applied potential for Zr-ZFO, TZF-5, TZF-15 and TZF-45 photoanodes respectively.

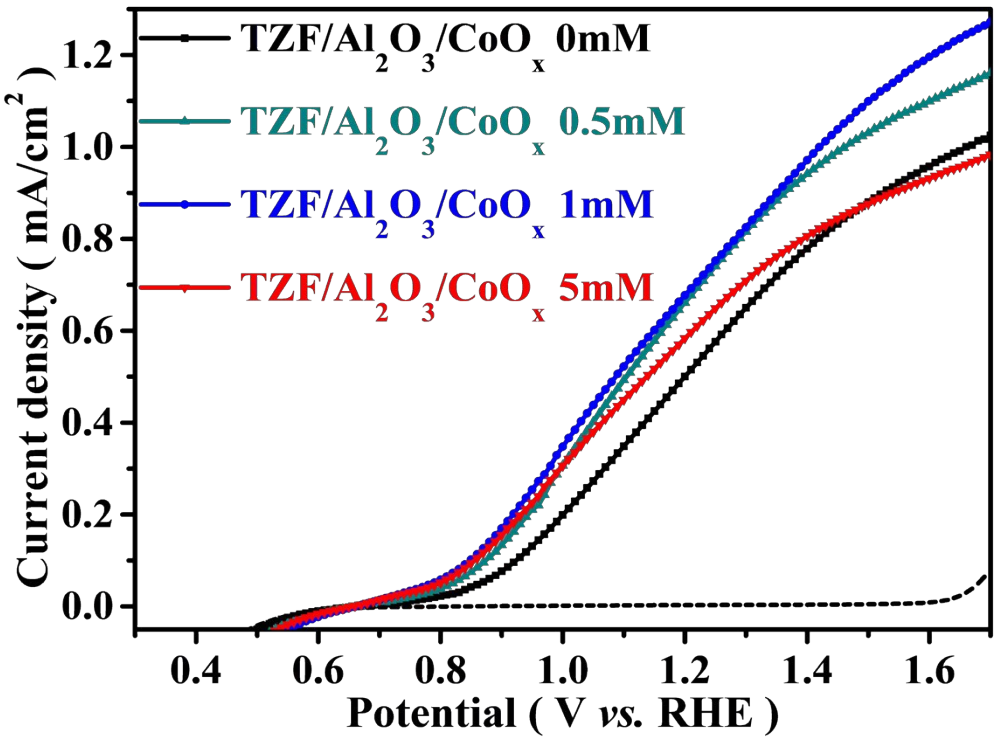

Fig. S7 Photocurrent density–potential characteristics under light (solid lines)/in the dark (dashed lines) conditions using 1 M NaOH for sample prepared with different concentration of cobalt precursor solutions; TZF/Al_2O_3/CoO_x_0mM, TZF/Al_2O_3/CoO_x_0.5mM, TZF/Al_2O_3/CoO_x_1mM and TZF/Al_2O_3/CoO_x_5mM.

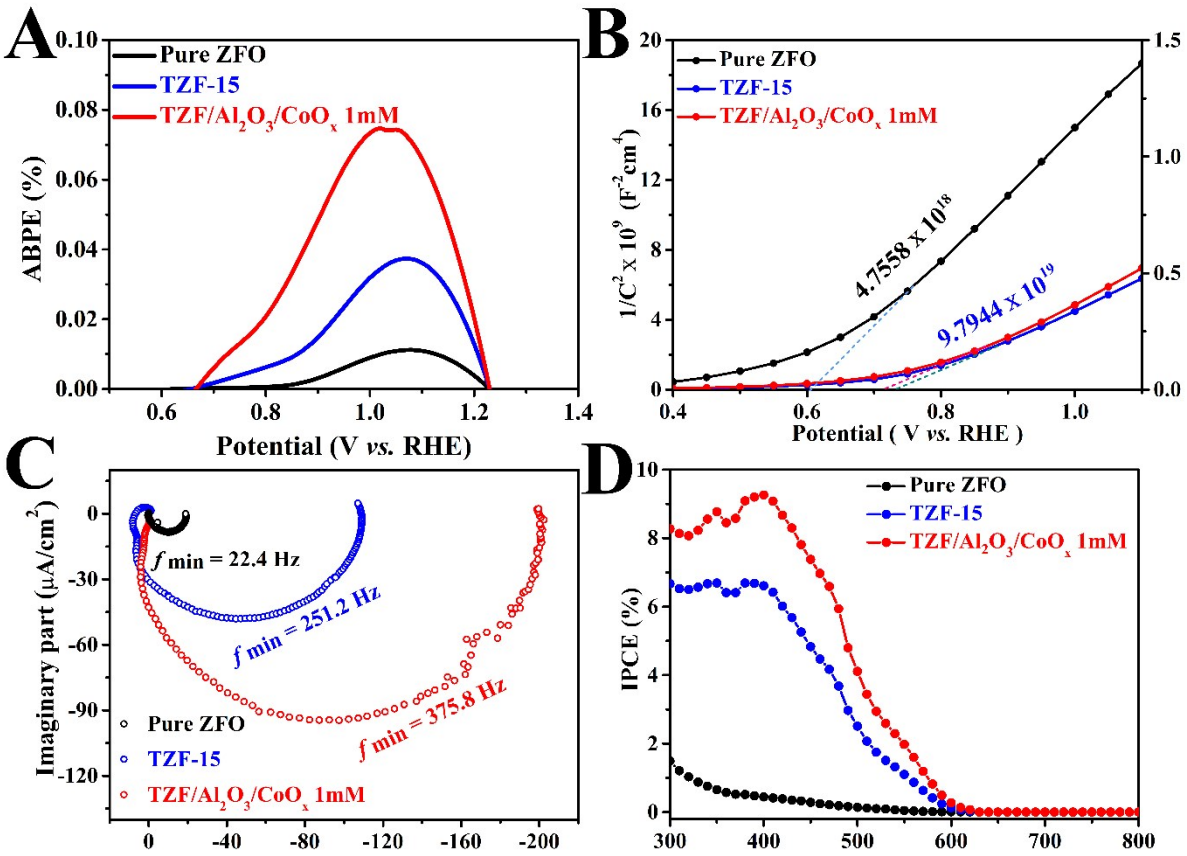

Fig. S8 (A) Photoconversion efficiency as a function of applied potential, (B) Mott–Schottky plots, (C) Complex plane plots of the IMPS response and (D) IPCE spectra of pure ZFO, TZF-15 and TZF/Al_2O_3/CoO_x_1mM photoanodes at 1.23 V vs. RHE using 1 M NaOH as electrolyte solution.

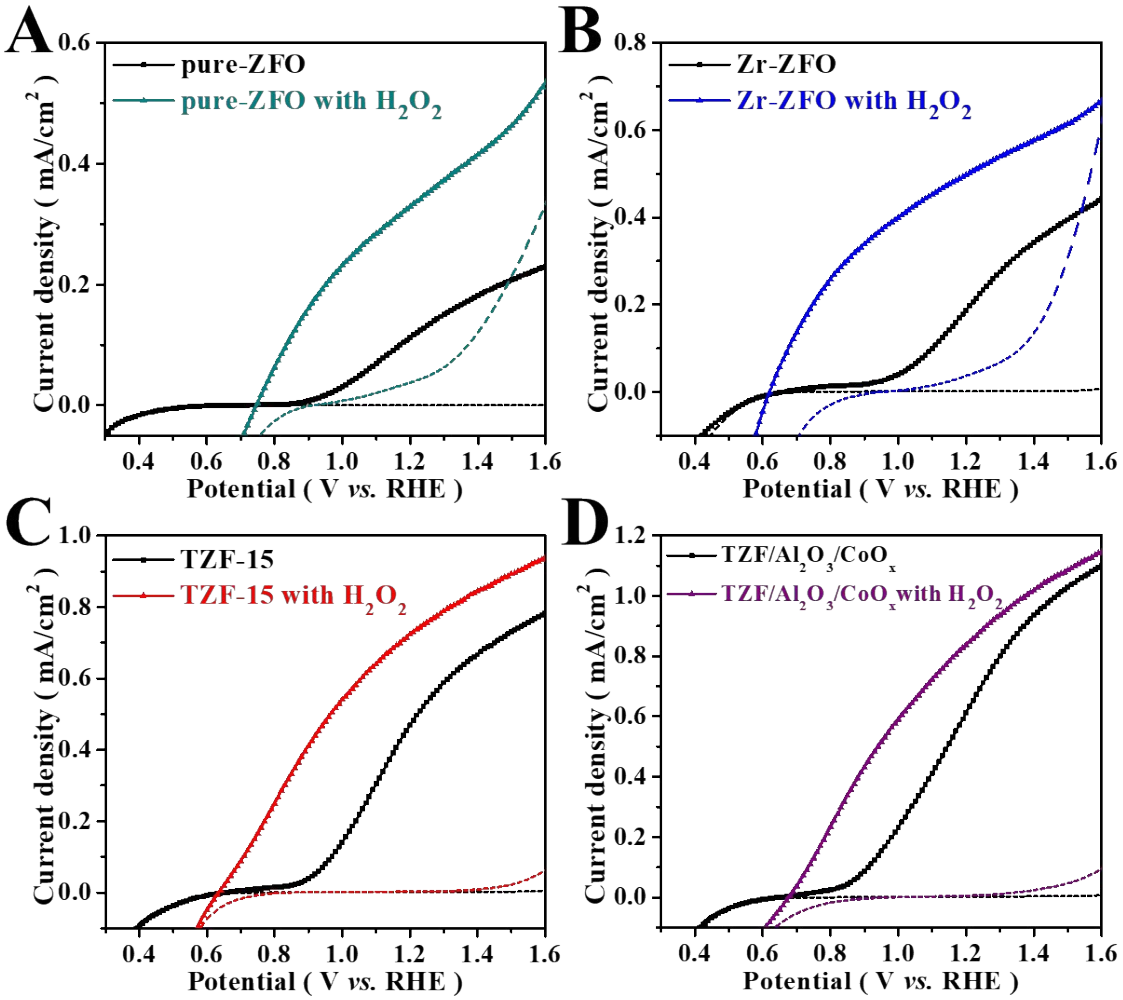

Fig. S9 Photocurrent density–potential characteristics of (A) pure ZFO, (B) Zr-ZFO, (C) TZF-15 and (D) TZF/Al_2O_3/CoO_x_1mM photoanodes under dark and illumination conditions using 1 M NaOH and 1 M NaOH + 0.5 M H_2O_2 with hole scavenger test.

Calculation of charge separation efficiencies: The charge separation efficiencies in the bulk (η_{bulk}) and on the surface ($\eta_{surface}$) of as-prepared photoanodes were measured by the addition of 0.5 M H_2O_2 as a hole scavenger in 1 M NaOH electrolyte solution. The $\eta_{surface}$ was calculated

by following equation: [1, 2]

$$J_{H2O} = J_{abs} \times \eta_{bulk} \times \eta_{surface} \quad \text{(S1)}$$

where J_{H2O} is the measured photocurrent density, J_{abs} is the photon absorption expressed as a current density (i.e., absorbed photon-to-current efficiency (APCE) = 100%).

With the addition of 0.5 M H_2O_2 as the electrolyte, the oxidation kinetics of the system is very rapid so that it largely suppresses the surface recombination of charge carriers without influencing the bulk charge separation, thus, $\eta_{surface}$ could be regarded as 100%. Therefore, η_{bulk}

and $\eta_{surface}$ can be determined by:

$$\eta_{bulk} = J_{H2O2} / J_{abs} \quad \text{(S2)}$$

$$\eta_{surface} = J_{H2O} / J_{H2O2} \quad \text{(S3)}$$

where J_{H2O} and J_{H2O2} are the photocurrent density measured in the 1 M NaOH electrolyte solution and the 1 M NaOH electrolyte solution with 0.5 M H_2O_2.

Tables

Table S1. EIS fitting parameters obtained from (a) pure ZFO and (b) pure ZFO with 15 mM TiO_2 underlayer photoanodes respectively, determined by fitting the experimental data using the equivalent circuit at 1.23 V *vs.* RHE.

Samples/ Parameters	R_s (Ω)	R_{CT1} (Ω)	R_{CT2} (Ω)	CPE1 (F)	CPE2 (F)
(a)	93	1684	409	1.95×10^{-5}	8.14×10^{-6}
(b)	87	2090	260	1.43×10^{-5}	2.76×10^{-6}

Table S2. Electron transport time results of the IMPS response for (a) Zr-ZFO, (b) TZF-5, (c) TZF-15 and (d) TZF-45 photoanodes respectively, at 1.23 V *vs.* RHE.

Samples	Frequency (Hz)	Electron transport time (μs)
(a)	126	1265
(b)	237	672
(c)	251	634
(d)	178	896

Table S3. PL lifetime parameters of (a) Zr-ZFO, (b) TZF-15 and (c) TZF-45 photoanodes.

Samples	A_1 (%)	τ_1 (ns)	A_2 (%)	τ_2 (ns)	A_3 (%)	τ_3 (ns)	$<\tau>^{a)}$ (ns)
(a)	85	0.30	14	1.1	1	5.6	0.47
(b)	98	0.17	2	2.0	-	-	0.21
(c)	89	0.23	10	1.2	1	30	0.62

Table S4. Atomic percent of the elements by X-ray Photoelectron Spectroscopy for (a) TZF-15 and (b) TZF/Al_2O_3/CoO_x_1mM photoanodes respectively.

Samples	Co (%)	Al (%)	Ti (%)	Zr (%)	Zn (%)	Fe (%)	O (%)	Sn (%)
(a)	0	0	1.21	3.000	4.96	24.56	66.12	0.16
(b)	1.08	1.87	1.27	5.90	2.08	20.13	67.50	0.17

Table S5. Comparative PEC activities and applications of $ZnFe_2O_4$ photoanodes prepared by different synthetic methods.

Photoanodes	Synthetic method	Morphology	Electrolyte	Performance (mA/cm^2 at 1.23 V *vs.* RHE)	Application	Stability [Ref.]
Synthesis of $ZnFe_2O_4$ and Co-catalysts	Hybrid microwave annealing and Co-Pi electrodeposition	Nanorods	1 M NaOH	0.24	PEC water splitting	180 min [3]
Sn-doped $ZnFe_2O_4$	Two-step hightemperature quenching	Nanorods	1 M NaOH	0.13	PEC water splitting	120 min [4]
Ti-doped $ZnFe_2O_4$	Spray pyrolysis	Nanoparticles	1 M NaOH	0.35	PEC water splitting	330 min [5]
Co-doped $ZnFe_2O_4$	All Solution based synthesis	Nanoparticles	-	-	Photodegradation (methylene blue)	- [6]
Synthesis of $ZnFe_2O_4$	Hydrogen treatment	Nanorods	1 M NaOH	0.32	PEC water splitting	180 min [7]
$ZnFe_2O_4$/ TiO_2 heterostructures	Solution-phase materials growth techniques and atomic layer deposition (ALD) step	Nanosheets/ Nanowires Heterostructures	1 M KOH	≈ 0.75	PEC water splitting	[8]
Dy-doped $ZnFe_2O_4$	Superficial chemical precipitation	Nanoparticles	-	-	Photodegrdation (methylene	- [9]

					blue)	
Cu-Sn dual doped $ZnFe_2O_4$	Chemical bath deposition	Nanorods	Nanorods 0.5 M Na_2SO_4	0.46	PEC water splitting	30 sec [10]
Synthesis of $ZnFe_2O_4$	Atomic layer Deposition	Nanorods	0.1 M NaOH	0.26	PEC water splitting	- [11]
Fe^{3+} self-doped spinel $ZnFe_2O_4$ with abundant oxygen vacancies $(Zn_{1-x}Fe_x)Fe_2O_{4-y}$	simple spincoating method, and subsequent hydrogen reduction treatment	worm-like nanoparticles	1 M NaOH	0.22	PEC water splitting	7 h [12]
Ti-doped $ZnFe_2O_4$ and Co-catalysts	Solution based hydrothermal method and $NiFeO_x$	Irregular nanorods	1 M KOH	0.312	PEC water splitting	360 min [13]
Nanorod array ZFO photoanodes	chemical bath deposition method and drop casting	Nanorods	1 M NaOH	0.8	PEC analysis	[14]
$NiFeO_x/TZFH_2$ photoanode	Hybrid microwave annealing	Irregular nanorods	1 M NaOH	0.91	PEC analysis	10 h [15]
TiO_2-underlayer *in-situ* Zirconium doped zinc ferrite nanocorals /Al_2O_3/CoO_x _1mM	**Simple solution method**	**Nanocorals**	**1 M NaOH**	**0.73**	**PEC water splitting**	**600 min [This study]**

Table S6. EIS fitting parameters obtained for (a) pure ZFO, (b) TZF-15 and (c) TZF/Al_2O_3/CoO_x_1mM photoanodes respectively, determined by fitting the experimental data using the equivalent circuit at 1.23 V *vs.* RHE.

Samples/ Parameters	R_s (Ω)	R_{CT1} (Ω)	R_{CT2} (Ω)	CPE1 (F)	CPE2 (F)
(a)	93	1684	409	1.95×10^{-5}	8.14×10^{-6}
(b)	65	410	120	1.59×10^{-4}	4.48×10^{-5}
(c)	69	424	108	1.81×10^{-4}	4.97×10^{-5}

Table S7. Electron transport time results of the IMPS response for (a) pure ZFO, (b) TZF-15 and (c) TZF/Al_2O_3/CoO_x_1mM photoanodes respectively, at 1.23 V *vs.* RHE.

Samples	Frequency (Hz)	Electron transport time (μs)
(a)	23	7108
(b)	251	634
(c)	376	424

References

[1] H. Dotan, K. Sivula, M. Graetzel, A. Rothschild, S.C. Warren, *Energy Environ. Sci*., 2011, **4**, 958-964.

[2] S. S. Yi, B. R. Wulan, J. M. Yan, Q. Jiang, *Adv. Funct. Mater*., 2019, **29**, 1801902.

[3] J. H. Kim, J. H. Kim, J. W. Jang, J. Y. Kim, S. H. Choi, G. Magesh, J. W. Lee, J. S. Lee, *Adv. Energy Mater*, 2015, **5**, 1401933.

[4] J. W. Park, M. A. Mahadik, G. W. An, S. Y. Lee, G. Piao, S. H. Choi, W. S. Chae, H. S. Chung, H. W. Park, J. S. Jang, *Sol. Energy Mater. Sol. Cells*, 2018, **187**, 207-218.

[5] Y. Guo, N. Zhang, X. Wang, Q. Qian, S. Zhang, Z. Li, Z. Zou, *J. Mater. Chem. A*, 2017, **5**, 7571-7577.

[6] G. Fan, J. Tong, F. Li, *Ind. Eng.,* 2012, **51**, 13639–13647.

[7] J. H. Kim, Y. J. Jang, J. H. Kim, J. W. Jang, S. H. Choi, J. S. Lee, *Nanoscale*, 2015,**7**, 19144-19151.

[8] X. L. Zheng, C. T. Dinh, F. P. G. Arquer, B. Zhang, M. Liu, O. Voznyy, Y. Y. Li, G. Knight, S. Hoogland, Z. H. Lu, X. W. Du, E. H. Sargent, *Small*, 2016, **12**, 3181-3188.

[9] P. A. Vinosha, S. Deepapriya, J. D. Rodney, S. J. Das, *AIP Conf. Proc*, 2018, **1942**, 050001.

[10] Y. Lan, Z. Liu, Z. Guo, M. Ruan, Y. Xin, *J. Colloid Interface Sci*., 2019, **552**, 111-121.

[11] A. G. Hufnagel, K. Peters, A. Muller, C. Scheu, D. Fattakhova-Rohlfing, T. Bein, *Adv. Funct. Mater.*, 2016, **26**, 4425.

[12] J. Wang, Y. Wang, X. Xv, Y. Chen, X. Yang, J. Zhou, S. Li, F. Cao, G. Qin, *Dalton Trans.*, 2019, **48**, 11934-11940.

[13] J. H. Kim, J. H. Kim, J. H. Kim, Y. K. Kim, J. S. Lee, *Solar RRL*, 2020, **4**, 1900328.

[14] X. Zhu, N. Guijarro, Y. Liu, P. Schouwink, R. A. Wells, F. L. Formal, S. Sun, C. Gao, K. Sivula, *Adv. Mater*. 2018, **30**, 1801612.

[15] J. H. Kim, Y. J. Jang, S. H. Choi, B. J. Lee, J. H. Kim, Y. B. Park, C. M. Nam, H. G. Kim, J. S. Lee, *J. Mater. Chem. A*, 2018, **6**, 12693-12700.